

Influence of Hydrogen Generation During Thermal Processes of Water Decomposition on the Surface of Nano- $\text{ZrO}_2+3 \text{ mol.}\% \text{Y}_2\text{O}_3$

¹Gunel Imanova, ^{2,3}Elmar Asgerov, ¹Sakin Jabarov, ⁴Mustafa Kaya, ²Aleksandr Doroshkevich

¹Department Of Physical, Mathematical And Technical Sciences, Institute Of Radiation Problems, Azerbaijan National Academy Of Sciences, AZ 1143 - Baku, Azerbaijan

²Joint Institute for Nuclear Research, 141980, Dubna, Moscow Region, Russian Federation

³National Nuclear Research Center CJSC, AZ1073, Baku, Azerbaijan

⁴Department of Chemical Engineering, Siirt University, Siirt, 56100, Turkey

Abstract. The physicochemical properties and crystal structure of nano- $\text{ZrO}_2+3 \text{ mol.}\% \text{Y}_2\text{O}_3$ were determined. The kinetics of the formation of H_2 as a result of the decomposition of H_2O on the surface of nano- $\text{ZrO}_2+3 \text{ mol.}\% \text{Y}_2\text{O}_3$ was studied. Effects of adsorption and desorption process on $\text{ZrO}_2+3 \text{ mol.}\% \text{Y}_2\text{O}_3$ nanoparticles were studied at different ($T=400\div 1000^\circ\text{C}$) temperature. The study of H_2 in thermal processes at nano- $\text{ZrO}_2+3 \text{ mol.}\% \text{Y}_2\text{O}_3$ system increased. Such an increase in H_2 generation in comparison with a pure H_2O as thermal processes had formed active centers for H_2O decomposition on the surface of the catalyst at the expense of δ -electrons emitted on the surface of nano- $\text{ZrO}_2+3 \text{ mol.}\% \text{Y}_2\text{O}_3$. This showed that the dimensions of the studied nanoscale particles systems are comparable to the free running distance of energy carriers generated by nano- $\text{ZrO}_2+3 \text{ mol.}\% \text{Y}_2\text{O}_3$ as a result of thermal processes. These results are promising for hydrogen generation by water splitting in near future.

Keywords: Nano- $\text{ZrO}_2+3 \text{ mol.}\% \text{Y}_2\text{O}_3$; Hydrogen generation; Kinetics; Thermal processes; Adsorption, Desorption.

1. Introduction

Recently, an interest of nuclear energy [1] has been increasing day by day due to the rapid increase in energy demand due to the rapid development of industry and the ineffectiveness of traditional methods, both economically and environmentally. Converting nuclear energy into a more affordable form of energy remains one of actual problem in the science and industry. It's known that porous materials in nano dimensions have excellent physical, physico-chemical and chemical properties with high specific surface area (more than $50 \text{ m}^2/\text{g}$). Therefore, these types of materials are widely used in different fields of science and technology. One of these areas of application is the method of obtaining molecular hydrogen from the decomposition of water used for the transition from nuclear energy to hydrogen energy using nanoscale and high surface area catalysts [3–8]. Three of these methods are preferred. The process is carried out both at the catalyst water boundary and with the solvated electrons emitted from the catalyst surface into the water in the system of nanoscale catalysts suspended in water at room temperature; in the third

method, the radiation-thermocatalytic processes of nanoparticles in contact with water vapor under the influence of temperature occur as the sum of two independent thermocatalytic and radiation-catalytic processes.

On the other hand, since silicon and its various compounds are used as construction materials inside the reactor [14], these materials are exposed to temperature and ionizing radiation (neutrons, protons, gamma rays, electrons) in contact with water and water vapor used as decelerators, retarders and energy carriers, α -particles, high-energy ions, etc.). Therefore, it is important to predict any changes in the operating mode inside the reactor, both for the safety of the reactor and for the transition to hydrogen energy in next-generation reactors. Nano catalysts have been created and utilized in water part with great accomplishments. The gamma radiation illumination of the water on the surface of nano catalyst increments the generation in hydrogen. It is known that the characteristic include of hydrogen generation forms in radiation-heterogeneous frameworks is the change of warm and ionizing radiation vitality into more efficient shapes in strong materials and, at last, hydrogen, which is the most vitality carrier in physicochemical forms. Nano auxiliary materials have a created surface and expanded deformity on the boundary of particles, which is of incredible noteworthiness in radiation-heterogeneous forms with their support, as well as amid the advancement of profoundly touchy locators of ionizing radiation. To modify physicochemical properties, materials based on the mixtures of nano sized oxides are produced [16].

Radiation-chemical yields of molecular products (H_2 , O_2 , H_2O_2 , etc.) from radiation-heterogeneous decomposition of water by metals or metal oxides used in each of these research methods are varies depending on their type, band-gap, particle size, saturation degree of adsorbed water on the particle surface, the temperature of the general system, the strength of the absorption dose, and the mass of metal or metal oxides suspended in the water [17].

The richness of water on the soil may be a huge advantage for us to produce hydrogen fuel. Hydrogen is made from water by water part utilizing different strategies. The critical strategies incorporate photocatalytic, photo-electrochemical, thermal deterioration and photo-biological radiolysis. Among these, photocatalytic of water is measured as the leading one due to green, effective, reasonable with consolation of prepare and with great volume of hydrogen shaped [16-18]. As a result of the getting and development of application capabilities of nano materials, measuring impacts gotten to be indeed more significant. In later a long time, the physical and chemical impacts of nano-dimensional frameworks, as well as their bizarre properties, have expanded intrigued within the ponder of these frameworks and the application of nano oxides in the field of radiation innovation has seriously nature.

Structural studies of zirconium nano particles have shown that monoclinus, tetragonal and cubic phases can be observed in this compound depending on the synthesis method [2, 9-10, 13,15].

The questions of conversion into the electric form of the energy of water molecules adsorption in 3 mol% Y_2O_3 doped ZrO_2 nanopowder systems were investigated using the density functional theory calculations. Based on the example of a nanopowder system ZrO_2 –3% mol Y_2O_3 with atmospheric humidity interaction, the possibility of exothermic heterophase electrochemical energy conversion to electric energy is shown [11-22].

Now the special attention to production of new technologies on production of dioxide of zirconium is paid. Dioxide of zirconium is used in metallurgy for receiving zirconium which is applied in nuclear reactors as constructional material.

In this work for the purpose of identification of zirconium dioxide influence on water surface, the kinetics of accumulation of molecular hydrogen at thermal processes of water in nano- ZrO_2 +mol.3% Y_2O_3 system at different temperatures $T = 400 \div 1000^\circ C$ is investigated.

2. Experimental:

2.1 Chemicals used:

The nanoscale zirconium dioxide was obtained from SkySpring Nanomaterials, Inc. 2935 Westhollow Dr., Houston, TX 77082, USA. The purity of nanoscale zirconium dioxide was 99.9% with $d = 10$ nm, density $\rho = 0.3$ g/cm³ and special surface area $S = 130$ m²/g. The density and size of nano- ZrO_2 are recorded in the passport of sample (by the Company).

2.2 Instruments used:

The instruments used were –

- Sample nano- ZrO_2 , USA.
- XRD-model number-"Bruker D8 Advance" Germany.
- Vacuum-absorption and desorption device- Azerbaijan.
- Gas chromatographs Agilent-7890A (USA).

2.3 Procedures

2.3.1 Surface area analysis

There are several methods used here, the most common of which are "particle size distribution", BET (Braunauer-Emmett-Teller) and Blain methods. One of the most accurate method, among of these is the "particle size distribution" method.

The SSA of nano ZrO_2 powder was calculated by this method. Assuming that all the particles are spherical, then we can calculate as follows. Thus, the volume of the $V_{spheres}$ and the surface area $S_{spheres}$ can be determined accordingly.

$$V_{sph.} = (\pi d^3)/6 \quad S_{sph.} = \pi d^2,$$

where d is the diameter of the sphere. The ratio of surface areas per volume is now calculated from these two equations

$$\frac{S_{sph.}}{V_{sph.}} = \frac{6}{d},$$

If we accept that the diameter of all the particles is up to d , then it can be defined as the volume of the total particles (where m is the total mass and ρ_n is the specific gravity of the sample). Using the volume of this particle, we can determine the total number of particles in the sample as follows

$$n = \frac{m_{smp.}}{\frac{\pi \cdot d^3}{6} \cdot \rho_n}$$

Hence, the specific surface area (SSA) of the sample can be calculated as follows

$$S = n \cdot S_{part.} = \frac{6 \cdot m_{smp.}}{d \cdot \rho_n}.$$

To achieve accurate SSA calculations particle sizes and shapes must be appropriate. In conclusion, it should be noted that in all cases, the calculations are performed with a certain accuracy and there are errors.

2.3.2 XRD Analysis:

The X-rays were done in the X-Ray Diffractometer D2 PHASER (model number-"Bruker D8 Advance") developed. For this reason, the scattered nanoparticles were arranged. This nanoparticulate chips was set within the goniometer of the diffractometer and the X-ray diffraction range of the test was drawn within the extend of diffraction point $20 < 2\theta < 100$. At that point on the premise of the gotten X-ray diffraction spectra the remove between the nuclear levelness (d), force of the gotten spectra, syngonia to which the test has a place, the cage measure, thickness, cage constants and spatial gather was decided. The cage parameters are calculated based on the square equations of crystallography.

2.3.3 Analysis gases:

Analysis of the amount of products (H_2 , CO_2) gases released in the gas phase during the the nano- $ZrO_2 + 3 \text{ mol\% } Y_2O_3$ system was carried out by chromatographic method Agilent-7890A

chromatograph).The analysis of hydrogen was performed on the US-made Agilent-7890A chromatograph in the following mode:

column: Carboxen-1010 PLOT, 30 m x 0.53 mm I.D. (25467)

Detector - TCD, "Constant Flow", Flow-3 ml / min,

20Hz / .01 min, T (head) = 50⁰C, T (detector) = 230⁰C

Makeup Flow = 0 ml / min,

gas carrier - Ar

oven: 50⁰C (7.0 min), 20⁰C / min to 230⁰C

injector temperature .: 230⁰C

2.3.4. Hydrogen generation:

Investigation of hydrogen and hydrogen-containing gasses in a vacuum adsorption and desorption gadget was carried out beneath static conditions. Exploratory thinks about were performed in uncommon quartz ampoules with a volume of $V=1\text{ cm}^3$ beneath static conditions. Sample of 10 nm zirconium dioxide were taken as the object of research. The ampoules were filling with the test of n-ZrO₂ = 1×10^{-3} g, at that point were closing in a vacuum adsorption and desorption gadget at a temperature of $T = 300\text{K}$ until $P = 10^{-2}$ Pa. In arrange to avoid oil and greases from falling on the tests three nitrogen-cooled holders are associated to the framework in vacuum-absorption and desorption device. Thermo-vacuum processing of samples is carried out with a zeolite pump at $T = 300\text{K}$, $P = 10^{-3}$ Pa for 2 hours. The gases generated were inhaled from each adsorbed and desorbed ampoule to the chromatograph directly.

3. Results and discussion

3.1 Chracterization

3.1.1 Surface area

Using the particle size distribution method, the specific surface area of the ZrO₂ nanoparticle size, was calculated and shown in Table 1.

Values of specific surface area of the nano-ZrO₂ sample

Sample	Nano-ZrO ₂ , <i>d</i> , nm	S _{spec} , m ² /g
n- ZrO ₂	10	130

The calculations show that the smaller the size, the larger the surface area. This means that the processes carried out on the sample take place not only on the surface but also in volume.

3.1.2 XRD analysis

The results of XRD analysis are shown in Figure 1.

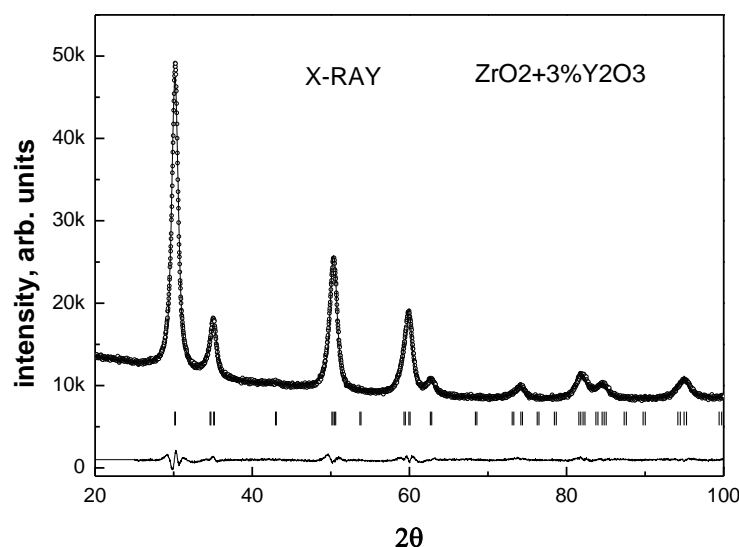


Figure 1: X-ray diffraction spectrum of the nano- $\text{ZrO}_2 + 3 \text{ mol. \% } \text{Y}_2\text{O}_3$ compound taken at the room temperature and in normal conditions

An X-ray analysis was carried out for a sample of $\text{ZrO}_2 + 3 \text{ mol. \% } \text{Y}_2\text{O}_3$ at room temperature on an X-Ray Diffractometer (XRD) D2 PHASER. The angular resolution of the survey was $\sim 0.01^\circ$. The X-ray diffraction data were processed by the Rietveld method using the FullProf program. The X-ray diffraction spectrum of $\text{ZrO}_2 + 3 \text{ mol\% } \text{Y}_2\text{O}_3$, obtained at room temperature, is shown in Fig 1. Under normal conditions, the diffraction spectra correspond to a tetragonal crystal structure with symmetry with the space group Pnma . The values of the unit cell parameters in this case were $a = b = 3.618 (2) \text{ \AA}$, $c = 5.161 (3) \text{ \AA}$ and (nano- ZrO_2 $a=5.1481 \text{ \AA}$, $b= 5.1962 \text{ \AA}$, $c=5.3132 \text{ \AA}$, $\beta=99.25^\circ$, $Z=4$ [2]) were in good agreement with the data of previous studies. The crystal structure of the sample was calculated by the equation $D = [K\lambda] / \beta \cos\theta$ [9,11,13].

3.2 Molecular hydrogen generation

In this work for the purpose of identification of zirconium dioxide influence on water surface, the kinetics of accumulation of molecular hydrogen at thermal processes of water in nano- $\text{ZrO}_2 + \text{mol.3\% } \text{Y}_2\text{O}_3$ system at different temperatures $T = 400 \div 1000^\circ\text{C}$ is investigated. Hydrogen occurrence kinetics during water thermal processes with the participation of nano- $\text{ZrO}_2 + \text{mol.3\% } \text{Y}_2\text{O}_3$ system are given in Figure 2-8. It is shown both: adsorption and desorption processes have been carried out in the nano- $\text{ZrO}_2 + \text{mol.3\% } \text{Y}_2\text{O}_3$ system and kinetic curves have been constructed.

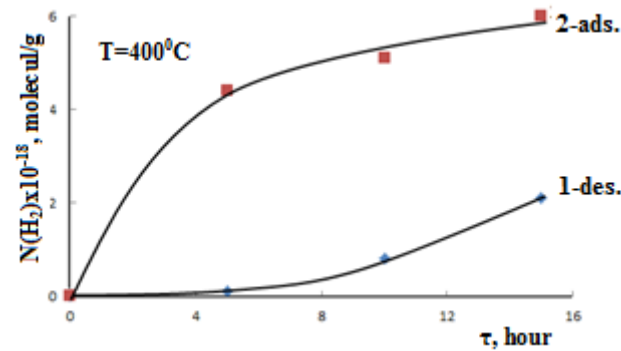


Figure 2: Kinetics of molecular hydrogen formation as a result of molecular thermal processes of adsorbed and desorbed water on nano-ZrO₂+mol.3% Y₂O₃ system, T=400°C

Figure 2 shows the adsorption and desorption curves on the nano-ZrO₂+mol.3% Y₂O₃ system surface, and these curves were calculated as a result of the values obtained in the analysis of gases.

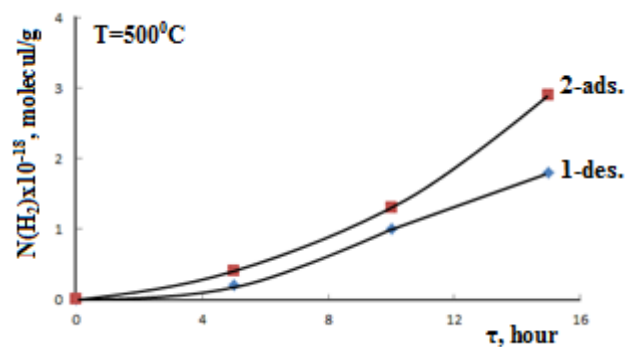


Figure 3: Kinetics of molecular hydrogen formation as a result of molecular thermal processes of adsorbed and desorbed water on nano-ZrO₂+mol.3% Y₂O₃ system, T=500°C

Figure 3 shows the adsorption and desorption curves on the sample surface. The curves shown in the graph show the results of adsorption and desorption processes.

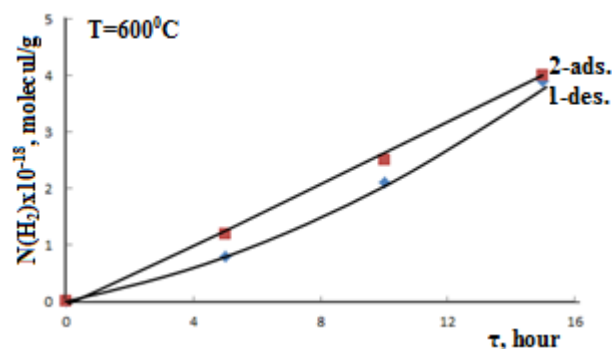


Figure 4: Kinetics of molecular hydrogen formation as a result of molecular thermal processes of adsorbed and desorbed water on nano-ZrO₂+mol.3% Y₂O₃ system, T=600°C

The values of the adsorption and desorption curves in Figure 4 are very close to each other, and these values are given in Table 2.

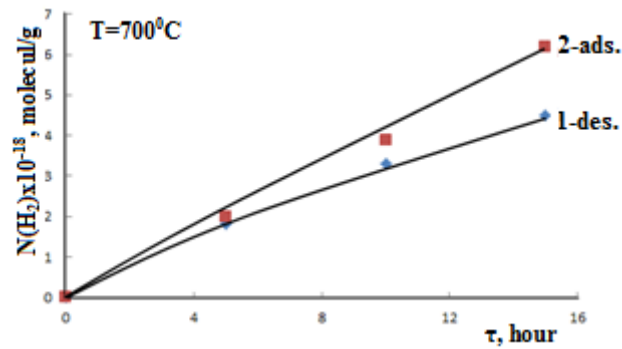


Figure 5: Kinetics of molecular hydrogen formation as a result of molecular thermal processes of adsorbed and desorbed water on nano-ZrO₂+mol.3% Y₂O₃ system, T=700°C

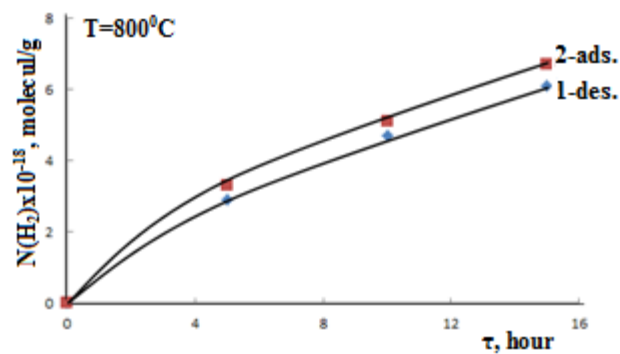


Figure 6: Kinetics of molecular hydrogen formation as a result of molecular thermal processes of adsorbed and desorbed water on nano-ZrO₂+mol.3% Y₂O₃ system, T=800°C

Figures 5 and 6 show that as the temperature increases in thermal processes, adsorption and desorption processes become more active. Each established kinetic curve was calculated for both processes and accurately plotted.

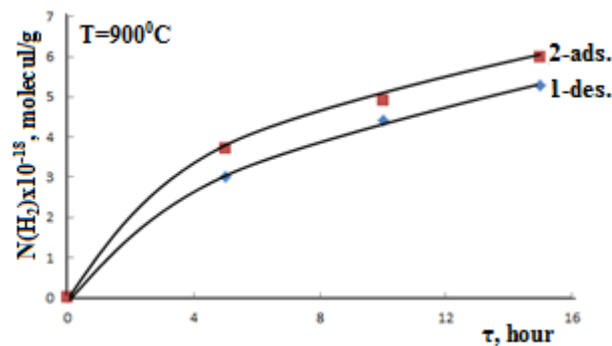


Figure 7: Kinetics of molecular hydrogen formation as a result of molecular thermal processes of adsorbed and desorbed water on nano-ZrO₂+mol.3% Y₂O₃ system, T=900°C

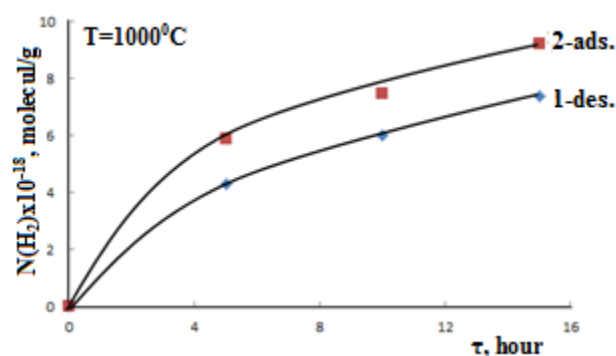


Figure 8: Kinetics of molecular hydrogen formation as a result of molecular thermal processes of adsorbed and desorbed water on nano-ZrO₂+mol.3% Y₂O₃ system, T=1000°C

In Figures 7 and 8, at the maximum value of the temperature, the formation of active centers on the surface is observed in both processes. A saturation state of 1000°C occurs and a stationary state begins to form here. That is, the higher the temperature, the more active the excitation on the surface, and this is clearly seen in both processes.

The speed of hydrogen were determined in the investigated system based on the based on the values obtained of the kinetic curves. The same results are given in Table 2.

Table 2: The speed of hydrogen were determined in the investigated system based on the based on the values obtained of the kinetic curves (nano-ZrO₂+mol.3%Y₂O₃) at different temperatures (T=400÷1000°C).

nano-ZrO ₂ +mol.3%Y ₂ O ₃						
N	Sample weight, g	Particle size, nm	Temperature, °C	Hour, τ	The speed of the process, W _T (H ₂)·10 ¹⁸ , molecule/g	
					desorption	adsorption
1	1·10 ⁻³	10	400	5	0,6	1,8
				10		
2				15		
			500	5	1,2	2,5
3				10		
				15		
			600	5	1,6	3,0
4				10		
				15		
			700	5	2,4	3,3
5				10		
				15		
			800	5	3,1	4,6
6				10		
				15		
			900	5	3,7	5,0
				10		

7				15	4,3	6,8
			1000	5		
				10		
				15		

The values of adsorption and desorption processes carried out in a thermal process at different temperatures ($T=400\div1000^{\circ}\text{C}$) are shown in Table 2. Table 2 shows that the values obtained in both processes are the values formed by the formation of active centers on the surface. Many physical and chemical processes have been observed here. Nanostructural materials possess a developed surface and increased defectness on the boundary of particles, which is of great importance in thermal proces with their participation, as well as during the development of highly sensitive catalizator of ionizing thermal. To modify physicochemical properties, materials based on the mixtures of nanosized oxides are produced.

Hence, the surface of oxide compounds is as a rule emphatically charged and have an electro-acceptor property. The concentration of surface electro-acceptor centers for diverse oxide compounds is decided by extraordinary tests and is in extend $L = 10^{12}-10^{13} \text{ sm}^{-2}$. These charged states ordinarily create an $E = 10^5-10^6 \text{ V/sm}$ electric field on the surface and influence the distinctive separations depending on the dielectric properties of the environment. Non-balanced charge carriers can relocate from oxide particles to the surface in two ways.

1. Diffusion, $x = \sqrt{D \cdot \tau}$, $x = 0.3-1.0 \text{ mcm}$.
2. Drift of charge carriers from volume to surface under the influence of a surface electric field (relative distance to the surface)

$$\mu = 40 \text{ sm}^2 / \text{V} \cdot \text{s}, \tau_{\text{max.}} = 10^{-10} - 10^{-3} \text{ s}, E = 10^5 - 10^6 \text{ V} / \text{sm}$$

$$d \approx 30 - 40 \text{ mcm}$$

Charge carriers on the surface level are recombined. As the scattering is diminished, the surrender of localized charge carriers diminishes.

Under the impact of the surface field, the charge carriers relocate from certain profundities (λ) on the surface in understanding with the appeared instruments. When shallow levels are not display, the particles in that volume are recombined and when surface levels are secured by an electro-water particle, the carriers are adsorbed and desorbed by them and the water particles are uncovered to thermal-catalytic forms. The nearness of water on the surface changes the charge state of the surface.

Obtained results can be explained based on the known mechanisms of radiation chemistry. The energy of Compton electrons are varies in the range of 0-1.02 eV depending on the scattering angle. Depending on their kinetic energy, the Compton electrons passes from the

nanoparticle several times into the liquid phase or vice versa, gradually losing their kinetic energies in both elastic and inelastic collisions and becoming thermal electrons in nano-ZrO₂ + 3% mol.Y₂O₃ system.

4. Mechanism

Under the influence of temperature, positively charged ions are formed in the defects in the catalyst as a result of the adsorption of water and the transfer of charges to water molecules. These positively charged ions cause the water molecules to disintegrate as a result of their recombination with the electrons formed on the surface. In this process, the production of hydrogen is determined by the cost of electrons and charges formed on the surface. As the temperature increases, the mobility of the particles on the surface of the catalysts increases. On the other hand, since part of the electron-hole pair involved in the decomposition of water is regenerated, these induced particles (by temperature) participate in the decomposition of water. Thus, the production of hydrogen at higher temperatures is greater.

5. Conclusions

The kinetics of hydrogen formation (a molecular product)via adsorbed and desorbed processes under the influence of thermal effect in the system of nano-ZrO₂ + 3% mol.Y₂O₃ is studied. In this process, water molecules are absorbed on the surface of nano-ZrO₂ + 3% mol.Y₂O₃. The speed of producing molecular hydrogen which ongoing in the nano surface at the thermal adsorption processes is 2.5 and 3 times higher than desorption. This showed when nano-ZrO₂+3%mol.Y₂O₃ was covered with water, the energy carriers (electrons, holes, excited states-excitons) formed under the influence of thermal effect in same system carried processes.

The checking of thermal effect initiated changes within the surface and the choice of the execution characteristic of as a heat-resistant catalytic fabric based on these nano materials. Thechanges in their physical and chemical properties made it conceivable to foresee the working modes of the catalytic materials. In this regard, it is of specific intrigued to study the changes within the surfaces of samples exposed to warm impact in comparison with the initial tests.

References

1. Basheer AA, Ali I. Water photo splitting for green hydrogen energy by green nanoparticles, Int. J. Hydro. Ener., 2019; 44: 11564-11572.
2. Imanova GT, Agayev TN, Jabarov SH. Investigation of structural and optical properties of zirconia dioxide nanoparticles by radiation and thermal methods, Modern Physics Letters B. 2020; 34: 2150050.

3. Imanova GT, Hasanov SH. Observation the initial radiation to the surface of mixed nano catalyst on oxidation processes, *International Journal of Scientific and Engineering Research*. 2020; 11: 869-873.
4. Imanova GT, Agayev TN, Garibov AA. Radiation-induced heterogeneous processes of water decomposition in the presence of mixtures of silica and zirconia nanoparticles, *High Energy Chemistry*. 2018; 52: 145-151.
5. Imanova GT, Garibov AA, Agayev TN. Radiation and catalytic properties on the $n\text{-ZrO}_2 + n\text{-Al}_2\text{O}_3$ systems in the process of hydrogen production from water, *Nanotechnologies in Russia*. 2017; 12: 22-26.
6. Agayev TN, Imanova GT, Musayeva ShZ. Studying the Kinetics of Formation of Molecular Hydrogen during the Radiolysis of Hexane and a Mixture of $\text{C}_6\text{H}_{14}\text{-H}_2\text{O}$ on a Surface of $n\text{-ZrO}_2$, *Russian Journal of Physical Chemistry A*. 2021; 95: 270–272.
7. Imanova GT, Agaev TN, Melikova SZ. Study of the radiation-thermal decomposition of water into nano- $\text{ZrO}_2 + \text{H}_2\text{O}$ by IR spectroscopy, *J. Chemistry of High Energy*. 2014; 48: 281-285.
8. Imanova GT, Agayev TN, Melikova SZ. An IR spectroscopic study of the effect of gamma radiation on the $n\text{-ZrO}_2 + n\text{-SiO}_2 + \text{H}_2\text{O}$ systems, *Surface Physicochemistry and Protection of Materials*. 2018; 54: 813-816.
9. Rezaei M, Alavi S, Sahebdehfar S, Xinmei L, Yan Z. Synthesis of mesoporous nanocrystalline zirconia with tetragonal crystallite phase by using ethylene diamine as precipitation agent, *Journal of Materials Science*. 2007; 42: 7086–7092.
10. Basahel S, Ali T, Mokhtar M, Narasimha K. Influence of crystal structure of nanosized ZrO_2 on photocatalytic degradation of methyl orange, *Nanoscale Research Letters*. 2015; 10: 73.
11. Mekhrdod Subhoni1, Kholmurzo Kholmurodov, Aleksandr Doroshkevich, Elmar Asgerov, Tomoyuki Yamamoto, Andrei Lyubchyk, Valer Almasan, Afag Madadzada Density functional theory calculations of the water interactions with ZrO_2 nanoparticles Y_2O_3 doped *Journal of Physics: Conf. Series* 994 (2018) 012013.
12. R.F. Hashimov, N.A. Ismayilova, F.A. Mikailzade, A.O. Dashdemirov, A.V. Trukhanov, S.V. Trukhanov, Y.I. Aliyev, E.B. Asgerov, S.H. Jabarov, N.T. Dang, Electronic structure and density of states in hexagonal BaMnO_3 , *Modern Physics Letters B*, 32, 2018, p.1850186.
13. Yashima M, Sasaki S, Kakihana M, Yamaguchi Y, Arashi H, Yoshimura M. Oxygen-induced structural change of the tetragonal phase around the tetragonal-cubic phase boundary in $\text{ZrO}_2\text{-YO}_{1.5}$ solid solutions, *Acta Cryst. B*. 1994; 50: 663-672.

14. Han Y, Zhu J. Surface Science Studies on the Zirconia-Based Model Catalysts, Topics in Catalysis. 2013; 56: 1525–1541.
15. A.S. Doroshkevich, E.B. Asgerov, A.V. Shylo, A.I. Lyubchyk, A.I. Logunov et al. Direct conversion of the water adsorption energy to electricity on the surface of zirconia nanoparticles Applied Nanoscience, 2019 pp 1-7.
16. LaVerne J, Tandon L. H₂ Production in the Radiolysis of Water on CeO₂ and ZrO₂, J. Phys. Chem. B. 2002; 106: 380–386.
17. LaVerne J. H₂ Formation from the Radiolysis of Liquid Water with Zirconia. J. Phys. Chem. B. 2005; 109: 5395–5397.
18. Caër S, Rotureau P. Radiolysis of Confined Water: Hydrogen Production at a High Dose Rate. ChemPhysChem. 2005; 12: 2585-2596.
19. Aleksandr S Doroshkevich, Elmar B Asgerov, Afag. I.Madadzada, Andrey I Lyubchyk, Akhmed K İslamov, Tatyana Yu Zelenyak, Artem V Shylo, Viktor I Bodnarchuk, Vitaliy A Turchenko, Maria Balasoiu Martensitic phase transition in yttrium-stabilized ZrO₂ nanopowders by adsorption of water 19th International Balkan Workshop on Applied Physics and Materials Science. July 16-19, 2019, Constanta, Romania. P. 161-162.
20. E.B. Asgerov, A.S. Doroshkevich, A.I. Madadzada, A.I. Beskrovnyy, E.P. Popov Martensitic phase transition in yttrium (0%, 3%, 8%)- stabilized ZrO₂ nanopowders by adsorption of water Twenty-first international summer school on vacuum, electron and ion technologies. 23-27 September 2019, Sozopol, Bulgaria
21. Asgerov E. Density functional theory calculations of the water interactions with ZrO₂ nanoparticles Y₂O₃ doped, Journal of Physics: Conference Series. 2018; 994: 012013.
22. Asgerov EB. The effect of percolation electrical properties in hydrated nanocomposite systems based on polymer sodium alginate with a filler in the form nanoparticles ZrO₂ - 3mol% Y₂O₃, Advanced Physical Research. 2019; 1: 70-80.